

**Chloramphenicol interaction with functionalized biochar in  
water: sorptive mechanism, fingerprinting effect and  
repeatable application**

Mohammad Boshir Ahmed<sup>a</sup>, John L Zhou<sup>a\*</sup>, Huu Hao Ngo<sup>a</sup>, Wenshan Guo<sup>a</sup>, Md Abu Hasan  
Johir<sup>a</sup>, Kireesan Sornalingam<sup>a</sup>, M. Sahedur Rahman<sup>b</sup>

<sup>a</sup>School of Civil and Environmental Engineering, University of Technology Sydney, 15  
Broadway, NSW 2007, Australia

<sup>b</sup>Department of Applied Chemistry and Chemical Engineering, University of Rajshahi,  
Rajshahi-6205, Bangladesh

Corresponding author:

Prof John L Zhou

School of Civil and Environmental Engineering

University of Technology Sydney

15 Broadway, NSW 2007

Australia

Email: junliang.zhou@uts.edu.au

## Abstract

Biochar and functionalized biochar (fBC-1 and fBC-2) were prepared and applied to remove antibiotic chloramphenicol from deionized water, lake water and synthetic wastewater. Results showed that chloramphenicol removal on biochar was pH dependent and maximum sorption occurred at pH 4.0-4.5. The sorption data of chloramphenicol fitted better with the Langmuir isotherm model than the Freundlich isotherm model with the maximum Langmuir sorption capacity of  $233 \mu\text{M g}^{-1}$  using fBC-2. Chloramphenicol sorption on fBC-2 followed the trend: deionized water > lake water > synthetic wastewater. The presence of humic acid decreased the sorption distribution coefficient ( $K_d$ ) while the presence of low ionic strength and soil in solution increased  $K_d$  value significantly. The mechanism of sorption on fBC mainly involved electron-donor-acceptor (EDA) interactions at pH < 2.0; formation of charge assisted hydrogen bond (CAHB) and hydrogen bonds in addition to EDA in the pH 4.0-4.5; and CAHB and EDA interactions at pH > 7.0. Additionally, solvent and thermal regeneration of fBC-2 for repeatable applications showed excellent sorption of chloramphenicol under the same condition, due to the creation of a fingerprinting effect in fBC-2. Consequently, fBC-2 can be applied with excellent reusability properties to remove chloramphenicol and other similar organic contaminants.

*Keywords:* Functionalized biochar; Chloramphenicol; Electron-donor interactions; H-bond; Reusability; Fingerprinting effect

## 1. Introduction

Antibiotics are widely produced and used in large quantities to treat diseases caused by microorganisms as they can selectively act on bacteria and pathogens without affecting human cells and tissues (Ahmed et al., 2015; Ahmed et al., 2017b; Boxall et al., 2003; Liao et al., 2013). Considering the different classes of antibiotics, chloramphenicols antibiotics have been commonly employed in veterinary clinics since the 1950s. Chloramphenicol, however, has geno-toxic effects and causes severe side effects such as aplastic anaemia, leukopenia, agranulocytosis and anaemia (Zhao et al., 2015). Although chloramphenicol has been banned since the 1990s in many countries for use in food-producing animals, it is still widely used due to its low cost and easy availability (Zhao et al., 2015; Nie et al., 2015). The occurrence and fate of chlorinated pollutants in the environment is recognized as an important problem due to the adverse effects on human health through the formation of emerging antibiotic-resistant bacteria and antibiotic-resistant genes (Mi et al., 2014; Chen et al., 2017). Low removal efficiencies of these organic contaminants have been reported through different biological treatment technologies (Ahmed et al., 2017a). Moreover, they are not easily degraded in the metabolite system and thus, they have been frequently detected in surface water, groundwater, and even in drinking water (Maskaoui and Zhou, 2010; Chen and Zhou, 2014). Several chemical methods have been applied to remove chloramphenicol from water (Lofrano et al., 2016; Nie et al., 2015; Wu et al., 2016; Xia et al., 2016). In addition, physicochemical methods have been applied for the removal of chloramphenicol (Dai et al., 2016; Fan et al., 2010; Qin et al., 2016; Zhu et al., 2016). Generally, adsorption by porous materials such as engineered activated carbon, resin, graphene oxide and carbon nanotubes is an expensive process. For this reason, biochar has received increasing interest due to its low cost (Ahmed et al., 2015), high hydrophobicity, aromaticity and multifunctional applications such as reduction of soil acidity, carbon sequestration and water remediation (Ahmed et al., 2016a; Chen et al., 2016; Dai et al., 2017; Das and Sarmah, 2015; Mandal et al., 2017; Sorrenti et al., 2016). However, biochar

properties depend on biomass origin, chemical composition, physical properties, and pre and post-treatment processes (Suliman et al., 2017). Biochar properties including surface functionality can be further improved through different modification methods (Ahmed et al., 2016b).

Adsorption of antibiotic onto biochar is expected to be heavily influenced by solution conditions and antibiotic speciation under different pH values (Ji et al., 2009a; Ji et al., 2009b; Ji et al., 2011; Taheran et al., 2016; Teixidó et al., 2011). Different species can interact with biochar through different mechanisms such as  $\pi$ - $\pi$  electron-donor-acceptor (EDA) interaction, nucleophilic addition, electrostatic attraction, cation bridging, cation/anion exchange, pore filling, partitioning into un-carbonized fraction and formation of the charge assisted hydrogen bond (CAHB) with surface oxygen groups (Liao et al., 2013; Teixidó et al., 2011). For example, during charcoal remove of tetracycline and chloramphenicol, Liao et al. (2013) found that  $\pi$ - $\pi$  EDA interaction, cation- $\pi$  bond in conjunction with hydrogen bonding interaction were the main mechanisms while surface diffusion was less likely to be involved. However, so far no studies clearly described the sorption behavior of chloramphenicol using carbonaceous materials such as carbon nanotubes, graphene or graphene oxide, and biochar. In addition, research is lacking on the potential regeneration and repeatable application of carbonaceous sorbents. The physicochemical properties of chloramphenicol are shown in **Table A.1**.

Therefore this study aimed to use biochar and fBC for removing chloramphenicol. Specifically the objectives were to (i) evaluate the interaction mechanism and performance of biochar and fBC for removing chloramphenicol; (ii) study the impact of humic acid, soil and salt concentrations on the sorptive behavior of chloramphenicol; (iii) assess the sorption performance in different water matrices for removing chloramphenicol; and (iv) examine the desorption and repeatable application of fBC with special emphasis on the fingerprinting effects during regeneration from different water.

## 2. Materials and methods

### 2.1. Chemicals

The standards of chloramphenicol (purity > 98%), potassium chloride, sodium chloride (> 99.6%), calcium chloride (> 97%), and organic solvents such as methanol, acetonitrile and formic acid of HPLC grade were purchased from Sigma-Aldrich, Australia. Peptone, beef extract, humic acid, tannic acid, sodium lignin sulphonates, Na-laryl sulphate, acacia gum powder, arabic acid, ammonium sulphate,  $K_2HPO_4$ ,  $NH_4HCO_3$ , and  $MgSO_4 \cdot 3H_2O$  were of analytical-grade. Phenanthrene (98%) and *para* amino benzoic acid (PABA, > 99%) were also purchased from Sigma-Aldrich. A Zorbax Bonus RP  $C_{18}$  column (5.0  $\mu m$ , 2.1  $\times$  1.50 mm) was purchased from Agilent Technologies. *Eucalyptus globulus* wood was donated by New Forest Asset Management Pty Ltd, Portland, Victoria, Australia. The soil sample was collected from the surface horizon (0-10 cm) at Willy Park, NSW, Australia. The soil was air dried, sieved (< 1.0 mm), and stored at room temperature for further use.

### 2.2. Preparation of biochar and fBC

Biochar and fBC were prepared according to our previous study (Ahmed et al., 2017b). Briefly, 50 g of bamboo or eucalyptus wood biomass was pyrolyzed at 380 °C at a heating rate of 10-11.4 °C min<sup>-1</sup> under nitrogen flow at 2.5 psi for 2 h, to obtain biochar samples coded BBC380 and EGBC380, respectively. Activation of BBC380 and EGBC380 was carried out through chemical activation method by soaking 15 g of each biochar in 30 mL of 50% ortho-phosphoric acid ( $oH_3PO_4$ ) for 3 h at 50 °C. The mixture was then heated at 600 °C for 2 h. After that, the prepared activated biochar was left to cool, washed and the pH adjusted to 7, followed by drying overnight at 100 °C, to obtain the activated biochar fBC-1 (prepared from bamboo) and fBC-2 (prepared from eucalyptus wood). Average biochar particles size ranged from 75 to 1000  $\mu m$ . As activated biochar was enriched with different functional groups (such as -COOH, -OH, C=O, C=C) on its surface, the prepared activated biochar was termed as fBC.

2.3. *Chloramphenicol sorption on biochar and fBC under different pH and different concentrations of humic acid, salt, soil and competitors*

Interactions of biochar and fBC with chlorinated chloramphenicol in deionized water were studied in batch method at different pH (1.6 to 9) to calculate  $K_d$ . Sorption was carried out in PTFE-lined screw cap glass vials with a capacity of 50 to 100 mL. Sorbents were pre-equilibrated at a specific pH followed by adding the required amount of sorbate solution with the same pH. Batch sorption isotherm experiments were conducted at pH ranging from 4.0 to 4.5 at 25 °C with initial chloramphenicol concentrations of 0.774 to 154.7  $\mu\text{M L}^{-1}$  at room temperature using 50-60  $\text{mg L}^{-1}$  of fBC and 100  $\text{mg L}^{-1}$  of biochar for 40 h. These conditions made it possible to calculate the maximum sorption at different pH values. The control experiments without sorbents were also executed.

To study the effects of salts, soil and humic acid on  $K_d$ , the sorption experiments were conducted by mixing humic acid or soil or salts with chloramphenicol (3.1  $\mu\text{M L}^{-1}$ ) overnight, before fBC-2 (being the best sorbent) was introduced. The sorption experiments were performed at pH 4.0-4.5 and 25 °C. Humic acid stock solution was prepared by dissolving the desired amount of humic acid in NaOH solution and stored for further use. Chloramphenicol sorption was also carried out in the presence of competitors (PABA and phenanthrene). The  $\pi$ -electron donor (phenanthrene) and  $\pi$ -electron acceptor (PABA) were chosen to unravel the possible EDA, electron acceptor-acceptor (EAA) and electron donor-donor (EDD) interactions mechanisms. The initial concentrations of chloramphenicol, phenanthrene and PABA were 3.1  $\mu\text{M L}^{-1}$ , 1.0  $\text{mg L}^{-1}$  and 1.0  $\text{mg L}^{-1}$ , respectively at different pH (~1.85, 4.0-4.5 and 9.0-10.5). Control experiments (no chloramphenicol) were also executed. The supernatant concentration of chloramphenicol and PABA were measured using HPLC with aliquots from each reactor being taken and filtered through a 0.2  $\mu\text{m}$  PTFE filter. Phenanthrene concentration was measured using UV-Vis spectroscopy.

## 2.4. Analytical method and data analysis

Chloramphenicol hydrolysis does not occur at pH 2–7 (Ahmed et al., 2017c). Its concentrations at different pH (1.7 to 11.0) were measured by HPLC (Jasco) equipped with an auto-sampler and UV detector at 285 nm, by 50 µL injection. A Zorbax Bonus RP C<sub>18</sub> column was used for the separation. Mobile phase A was composed of acetonitrile and formic acid (v/v, 99.9: 0.1) while mobile phase B was composed of Milli-Q water and formic acid (v/v, 99.9: 0.1). The elution used 40% of A and 60% of B at a flow rate of 0.4 mL min<sup>-1</sup>, which was changed to 0.3 mL min<sup>-1</sup> at 0.1 min. The method run time was 7 min. The same method was used for the measurement of PABA concentration with HPLC. Phenanthrene concentration was measured using UV-Vis spectroscopy (Shimadzu, UV-1700) at ~251 nm. In addition, the concentration of Ca<sup>2+</sup> and Cl<sup>-</sup> were measured using a Merck Spectrophotometer (NOVA 60) and relevant test kits.

The adsorption data were fitted to the Langmuir and Freundlich models. The apparent sorption distribution coefficient ( $K_d$ , L kg<sup>-1</sup>) is defined as the ratio of adsorbate sorbed per unit sorbent mass ( $Q_e$ , µM g<sup>-1</sup>) to adsorbate concentration in solution ( $C_e$ , µM L<sup>-1</sup>) at equilibrium, and was calculated using equation (1):

$$K_d = 1000 \frac{Q_e}{C_e} = 1000 \left( \frac{C_o - C_e}{C_e} \right) \frac{V}{M} \quad (1)$$

where  $C_o$  is the initial adsorbate concentration in water (µM L<sup>-1</sup>),  $V$  is the solution volume (L) and  $M$  (g) is the sorbent mass.

The Langmuir and Freundlich isotherm models can be represented as follows:

$$\text{Freundlich model: } Q_e = K_F C_e^{1/n} \quad (2)$$

$$\text{Langmuir model: } Q_e = \frac{Q_{max} K_L C_e}{1 + K_L C_e} \quad (3)$$

where  $Q_{max}$  is the maximum adsorption capacity (µM g<sup>-1</sup>),  $1/n$  is a dimensionless number related to surface heterogeneity,  $K_F$  is the Freundlich capacity-affinity coefficient (µM<sup>1-n</sup> L<sup>n</sup> g<sup>-1</sup>) and  $K_L$  is the Langmuir fitting parameter (L µM<sup>-1</sup>). Parameters were estimated by nonlinear regression

weighted by the dependent variable using above equations and fitting in Origin pro software (version 2016).

## 2.5. Characterizations of the sorbents

Characterization of the prepared materials was carried out using Scanning Electron Microscope with Energy Dispersive Spectrometer (SEM-EDS) (**Table A.2**), Brunauer-Emmett-Teller (BET) analyzer, Raman spectroscopy and Fourier transform infrared spectroscopy (FTIR). Raman shifts measurement was done using Renishaw in Via Raman spectrometer (Gloucestershire, UK) equipped with a 17 mW Renishaw Helium-Neon Laser 633 nm and CCD array detector at 50% laser intensity. Structural analysis was conducted using FTIR (Miracle-10; Shimadzu). The spectra were obtained at 4 cm<sup>-1</sup> resolutions by measuring the absorbance from 400 to 4000 cm<sup>-1</sup> using a combined 40 scans. The specific surface area and the porosity distributions were calculated using BET nitrogen adsorption-desorption isotherms and the Barrett-Joyner-Halenda (BJH) method, respectively by using a Micromeritics 3 Flex<sup>TM</sup> surface characterization analyzer at 77 K. Zeta potential was measured twice using 1.0 mM KCl solution at different pH for 48 h (Nano-ZS, Malvern). Zeta potential was measured twice for each pH.

## 2.6. Desorption and regeneration of fBC-2

Desorption experiments were conducted in different water matrices to calculate desorption percentage of chloramphenicol, [study on fingerprinting effects](#) and the reusability of the sorbent (fBC-2). After experiments, the supernatant was decanted and replaced with an equal volume of 50% methanol. The fBC-2 and the solution mixture were shaken on an orbital shaker for 24 h at 120 rpm and the suspension was centrifuged for 7 min at 2000 rpm. The supernatant was then filter using 0.2 µm PTFE filter paper and chloramphenicol concentration was measured



using HPLC. Desorption was performed after each sorption cycle using fBC-2. The thermal regeneration and fingerprinting ability of fBC-2 was examined by heating fBC-2 at 300 °C.

## 2.7. Water and wastewater samples

Synthetic wastewater was prepared based on a recent study (Ahmed et al., 2017c) (Table A.3) and lake water was collected from Victoria Park, NSW, Australia. All water samples were filtered through 1.2 µm filter paper and stored in a fridge. The characteristics of lake water are given in Table A.3. Deionized water, lake water and synthetic wastewater were spiked with 3.10 µM L<sup>-1</sup> chloramphenicol and contacted with fBC-2 to examine sorption trends in different water. Control experiments were also conducted.

## 3. Results and discussion

### 3.1. Sorbents surface properties

Surface properties of biochar and fBC were carried out using BET, EDS, FTIR, Raman and zeta potential measurement. EDS data showed that BBC380 comprised of mainly ~81% C and ~19% O while fBC-1 comprised of 59% C, 28% O, ~5% N and ~8% P, with O/C molar ratio of 0.363. The fBC-2 was composed of 60.8% C, 25.4% O, ~5% N and ~8% P, with O/C molar ratio of 0.314 (Table A.2). BET surface area of fBC-1 and fBC-2 were found to be 1.12 and 1.18 m<sup>2</sup> g<sup>-1</sup>, respectively. The Langmuir surface area of fBC-1 and fBC-2 was 7.23 and 8.22, respectively. The pore size distribution of fBC-1 and fBC-2 is represented in Fig. A1. FTIR peak of each EDC is shown in Fig. 1. All biochar had alkyl -C-C- groups, aromatic -C=C- group (due to conjugated arene units), ketonic or carboxylic -C=O group and at least one hydroxyl functional group (alkyl or phenolic -OH) in its structure. The peaks around 3300-3850 cm<sup>-1</sup> represents the presence of hydroxyl groups whereas peaks at 2926-2976 cm<sup>-1</sup> represent the asymmetric carbon. In addition, two characteristics peaks at 1720 cm<sup>-1</sup> and 1520-

1594  $\text{cm}^{-1}$  represent the presence of  $-\text{C}=\text{O}$  and  $-\text{C}=\text{C}-$  groups (Ahmed et al., 2016b; Ahmed et al., 2017c).

Raman spectroscopy was also carried out to obtain further data on fBC before and after sorption. fBC showed two characteristic peaks at 1592-1597 and 1325-1345  $\text{cm}^{-1}$  (**Fig. 1b**). The two broad peaks located at  $\sim 1325\text{-}1345\text{ cm}^{-1}$  and  $\sim 1592\text{-}1597\text{ cm}^{-1}$  corresponded to the D-band (disordered structure) and G-band (graphitic structures) of  $\text{sp}^2$ -type carbon presence in fBC (Peng et al., 2016). The sharp and relative band intensity ratio ( $I_G/I_D$ ) showed the degree of functionalization in biochar. It is important to note that Raman spectra of fBC featured a strong D-band, which illustrated a slightly more amorphous character (disordered) of the carbon in fBC (Pang et al., 2016). D-band surface defect was possible by the introduction of other elements onto carbon structure during fBC preparation.

### 3.2. Chloramphenicol $K_d$ on biochar and fBC

Chloramphenicol sorption on biochar, fBC-1 and fBC-2 revealed pH dependence. The effect of pH on the sorption coefficient is shown in **Fig. 2**. Clearly, chloramphenicol sorption was greatly governed by the electrostatic interactions between chloramphenicol and fBC surfaces. The maximum  $K_d$  value for biochar (BBC380) was found to be  $\sim 500\text{ L kg}^{-1}$  at pH around 4.5. **Similar result was obtained for EGBC380 (data not shown).** However, higher  $K_d$  values were observed for both fBC-1 and fBC-2 than biochar at all pH values studied. The finding indicated that functionalization of biochar significantly changed the biochar properties and increased its sorption capacity. The  $K_d$  values for both fBC reached their first maxima at pH  $\sim 1.6$  and the maximum at approximately pH 4.5. A further increase in pH resulted in decreasing  $K_d$  values. Detailed mechanism in relation to pH values are discussed in section 3.4. Based on the results, the maximum  $K_d$  values were found to be  $\sim 1.8 \times 10^4\text{ L kg}^{-1}$  for fBC-2 and  $\sim 1.2 \times 10^4\text{ L kg}^{-1}$  for fBC-1 at pH  $\sim 4.0\text{-}4.5$  with initial chloramphenicol concentration of  $15.5\text{ }\mu\text{M L}^{-1}$ . As fBC-2

showed a higher  $K_d$  value than fBC-1 for chloramphenicol, it was used in further sorption experiments.

### 3.3. Effects of humic acid, salt and soil concentration on $K_d$

The effect of humic acid on  $K_d$  was studied using different concentrations of humic acid (1.0 to 40.0 mg L<sup>-1</sup>). It emerged that the increase of humic acid concentration from 1.0 mg L<sup>-1</sup> to 10 mg L<sup>-1</sup> reduced  $K_d$  value slightly from  $\sim 2.0 \times 10^4$  to  $\sim 1.7 \times 10^4$  L kg<sup>-1</sup> (**Fig. 3a**). A further increase in humic acid concentration caused a significant reduction in the  $K_d$  of chloramphenicol which fell sharply to  $\sim 6.1 \times 10^3$  L kg<sup>-1</sup> when humic acid concentration was raised to 40 mg L<sup>-1</sup> (**Fig. 3a**). In comparison, the  $K_d$  value in deionized water, in the absence humic acid, under the same initial conditions was  $\sim 6.9 \times 10^4$  L kg<sup>-1</sup> (SD,  $3.7 \times 10^3$ ). This indicated that humic acid yielded a negative influence on the sorptive removal of chloramphenicol which can be explained by the direct competition of humic acid and fBC sorption sites for the sorption of chloramphenicol (Zhang et al., 2015; Pignatello et al., 2006). Pignatello et al. (2006) found that natural organic substances (e.g. humic substances) appear partially block biochar pore network and may suppress adsorption by a competitive effect at the external surface at normal temperature. The strongest suppression occurs for large molecules with reduced access to interior pores, especially when the biochar has been co-flocculated with the humic substance. Moreover, Zhou et al. (2015) confirmed that pore blockage (confirmed by BET surface area measurement) as well as the more hydrophilic surface with more sorbed water molecules mainly suppressed the sorption of atrazine by biochar. In addition, hydrophobic effects and electron donor acceptor (EDA) might also be responsible for lower chloramphenicol sorption in the presence of humic acid. Hence, the presence of humic acid decreased sorption of chloramphenicol which was significant when the humic acid concentration was more than 20 mg L<sup>-1</sup>.

The presence of lower ionic strength increased  $K_d$  slightly (**Fig. 3b**). For example, in the presence of 0.001 M NaCl,  $K_d$  was found to be  $\sim 7.0 \times 10^4$  L kg<sup>-1</sup> (initial chloramphenicol

concentration was  $3.1 \mu\text{M L}^{-1}$ ), whereas it was  $\sim 6.9 \times 10^4 \text{ L kg}^{-1}$  in the absence of salt with the same initial chloramphenicol concentration. This effect can be explained by the ionic mobility. Lower ionic strength increased the ionic mobility of a solution hence the ionic mobility of the fBC was increased and contributed to the overall increase in sorption (Park et al., 2008). However, a further increase in ionic strength (i.e. NaCl concentration up to 0.01 M) slightly decreased the sorption distribution efficient. Further increase of NaCl concentration (0.10 M) did not have significant effect on the sorption of chloramphenicol and the  $K_d$  was almost same. This can be explained by the saturation of biochar surface in the presence of a higher concentration of NaCl. On the other hand, in the presence of low calcium chloride concentration (0.001 M), the  $K_d$  values was almost the same as that without  $\text{CaCl}_2$ . However, further increase in  $\text{CaCl}_2$  concentration (up to 0.01 M) reduced the  $K_d$  values linearly, indicating that sorption of chloramphenicol in the presence of excess  $\text{CaCl}_2$  salt had much higher negative influence than that of NaCl (**Fig. 3b**). Control experiments with only  $\text{Ca}^{2+}$  showed that  $\text{Ca}^{2+}$  was sorbed by fBC-2 (initial  $\text{Ca}^{2+}$  concentration =  $155 \text{ mg L}^{-1}$ , final concentration =  $146.5 \text{ mg L}^{-1}$ ) at pH  $\sim 4.45$ . Thus, it can be stated that biochar surface was highly saturated by salt of divalent calcium ion as this ion which contributes to water hardness like magnesium.

Furthermore,  $K_d$  value was found to be significantly higher in the presence of soil, e.g.  $1.06 \times 10^5 \text{ L kg}^{-1}$  in the presence of  $5.0 \text{ mg L}^{-1}$  of soil (50-60  $\text{mg L}^{-1}$  of fBC-2 dosage). While in the absence of soil, chloramphenicol sorption  $K_d$  value was  $\sim 6.9 \times 10^4 \text{ L kg}^{-1}$  (SD  $3.7 \times 10^3$ ). It is usual that biochar adsorbs organic contaminants significantly more than soil, and the addition of biochar to soil significantly increases sorption capacity which also depends on the type of soil (Cornelissen and Gustafsson, 2005; Lahmann and Joseph, 2015). Soil solids consist of different minerals (e.g. quartz, calcite, montmorillonite, iron oxide) and organic matter (e.g. biopolymers, microbial and root exudates, plant litter in varying stages of degradation). Pure clay minerals and metal oxides have highly reactive surfaces, in most soils, coating/modifying of soil surfaces by organic matter profoundly modifies their sorptive character. As a result, soil

organic matter fraction governs the sorption of virtually all organic molecules in soil (Lahmann and Joseph, 2015). Thus, the increase in  $K_d$  values might be due to soil organic matter and different minerals which make contribution to the overall sorption of chloramphenicol onto fBC-2. From literature it is found that, soil organic matter ( $\pi$ -electron acceptor site) can interact with an aromatic organic compound (with  $\pi$ -donor site) through  $\pi$ -electron donor acceptor interactions (Zhu et al., 2004) which might happen in this case. Yet, the increase in soil concentration (up to  $1.0 \text{ g L}^{-1}$ ) with the same dosage of fBC-2 reduced  $K_d$  values, indicating that fBC-2 dominated the overall sorption compared to soil. An increase in the amount of soil led to a decline in  $K_d$  values which may be due to partial deposition of soil particles onto biochar active surface that might block or hinder the pores of the fBC-2 as well as due to release of more organic matter including minerals in the solution (**Fig. 3c**). This aligns with the finding of different ionic strength solution discussed earlier in this section. However, chloramphenicol adsorption was still significant which was mainly due to the sorption by fBC-2 with partial contribution from soil minerals and organic fractions.

### 3.4. Affinity and mechanism of chloramphenicol sorption by fBC

The sorption data was better fitted to the Langmuir isotherm model than the Freundlich model (**Fig. 4a**). The maximum Langmuir adsorption capacities ( $Q_{max}$ ) were found to be 26.2, 200.5 and  $233 \text{ } \mu\text{M g}^{-1}$  for biochar, fBC-1 and fBC-2, respectively. Conversely, the maximum Freundlich constant ( $K_F$ ) values were 1.6, 39 and  $56 \text{ } \mu\text{M}^{1-n} \text{ L}^n \text{ g}^{-1}$  for biochar, fBC-1 and fBC-2, respectively (**Table 1**). The higher adsorption by fBC-2 was attributed to change in the specific surface area, microspore volume, and the introduction of additional sites onto fBC through different interactions (Ahmed et al., 2015; Ahmed et al., 2017b). Further,  $K_d$  values varied between  $1.0 \times 10^2$  and  $1.6 \times 10^3$ ;  $1.35 \times 10^3$  and  $8.0 \times 10^4$ ; and  $1.6 \times 10^3$  and  $1.2 \times 10^5 \text{ L kg}^{-1}$  for biochar, fBC-1 and fBC-2, respectively (**Fig. 4b**). The isotherm showed little sign of becoming linear at lower end of the experimental concentration range for BBC380 ( $1/n = 0.50$ ) than that

of fBC-1 ( $I/n = 0.34$ ) and fBC-2 ( $I/n = 0.30$ ), upon regressing data from 0.774 to 154.74  $\mu\text{M}$   $\text{L}^{-1}$  of chloramphenicol (**Fig. 4a**). The observed values of  $K_d$ ,  $Q_{\text{max}}$  and  $K_F$  for chloramphenicol were higher than reported values (Ji et al., 2009b; Liao et al., 2013). For example, biochar prepared at 400-700 °C from bamboo (Liao et al., 2013) had a Langmuir sorption capacity of 25.11  $\mu\text{M g}^{-1}$ . The detailed sorption mechanisms at different pH are described in more detail below.

#### ***At pH below 2.0***

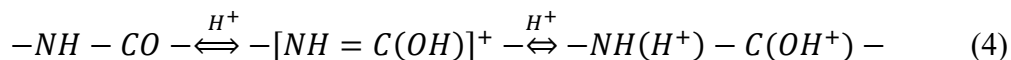
At low pH, higher  $K_d$  values were obtained (**Fig. 2**). At very low pH, proton exchange from surface functional groups (-OH and -COOH) of the biochar is not possible due to the higher  $pK_a$  values of the surface hydroxyl group (7-10) and surface -COOH group (4.0-5.0) (Pan et al., 2008). Thus, if solution pH could be maintained near the  $pK_a$  value, then proton exchange might contribute to the sorption process. This suggests that proton exchange is not favorable at low pH and subsequently, maximum sorption of chloramphenicol may be mostly due to EDA interactions with  $\pi$ -electron rich biochar and chloramphenicol surface (Ma et al., 2016; Teixidó et al., 2011). It is assumed that stronger EDA interactions between oppositely polarized quadrupoles might be possible when the  $\pi$ -electron depletes aromatic rings (or regions) and  $\pi$ -electron rich regions (or aromatic rings) interact each other. fBC was enriched with C=C, -OH, C=O and -COOH groups (**Fig. 1**) and surface zeta potential was +2.20 to +2.50 (point of zero charge) (**Table A.4**). The surface functional groups of fBC may act as a strong  $\pi$ -electron-donor due to (i) hydroxyl groups being situated in the benzene rings (participating in resonance as a  $\pi$ -electron donor), and (ii) strong  $\pi$ -electron-acceptors due to carboxyl functional groups/ ketonic functional groups on the benzene rings (Ahmed et al., 2017b; Keiluweit and Kleber, 2009; Lattao et al., 2014; Sander and Pignatello, 2005; Zhu and Pignatello, 2005; Zhu et al., 2005). Thus, when the  $\pi$ -electron-acceptor is positively charged and this charge lies within or resonates with an arene unit of chloramphenicol then a stabilized overall interaction is designed as  $\pi$ - $\pi$  EDA. Resonance forms of positive species of chloramphenicol are able to form  $\pi^+$ -

electron (acceptor site) and sorption affinities are mostly governed by the mechanism of  $\pi$ - $\pi$  EDA (**Case I, Fig. 5**) (Ahmed et al., 2017b). In addition, electron acceptor-acceptor (EAA) interactions (**Case II, 1<sup>st</sup> part**) may also be possible but not critical.

To test the  $\pi$ - $\pi$  EDA hypothesis, the competitive effects of two compounds having similar affinity for the surface but opposite quadrupolarity were compared: phenanthrene, a  $\pi$ -electron donor by virtue of its  $\pi$  rich electrons (polarizable ring system) and PABA, a strong  $\pi$ -electron acceptor by virtue of the withdrawing capability of the acid groups. The results are presented in Figs **6a and 7**. It can be predicted that their competitor's strengths against chloramphenicol sorption would be similar if the competitive effect was due merely to nonspecific forces, whereas PABA would be a much stronger competitor than phenanthrene if the  $\pi$ -electron acceptor property of chloramphenicol as well as  $\pi$ -electron donor property of fBC arene units were critical. Figs 6a and 7 clearly show that PABA strongly interacted with fBC-2 (i.e. with graphene like arene unit as  $\pi$ -electron donor site), suppressing chloramphenicol (acted as  $\pi$ -electron acceptor) adsorption significantly than phenanthrene (acted as  $\pi$ -electron donor). Thus, PABA is, by far, the stronger competitor than phenanthrene for chloramphenicol sorption (Fig. 6a). This kind of interactions can be written simply as  $\pi$ -  $\pi$  EDA interactions, where EDD interactions were not as strong as EDA interaction. *As the sorption of chloramphenicol was increased by ~10% (excluding SD) in the presence of phenanthrene indicating the insignificant role of EDD interactions.* Similar explanation can be drawn in the absence of chloramphenicol where adsorption of PABA was higher than that in the presence of chloramphenicol (Fig. 7). Moreover, cation exchange capacity of fBC-2 ( $\text{Ca}^{2+}$ ) in this pH range was excluded as  $\text{Ca}^{2+}$  ion adsorption capacity was found to be insignificant (data not included). We also observed, anion competitor such as  $\text{PO}_4^{3-}$  can reduce chloramphenicol sorption capacity by ~8 % at this pH range and thus anion exchange capacity of fBC-2 might be important under this condition.

Besides, the maximum  $K_d$  values can also be partially attributed to the degradation nature of chloramphenicol in excess hydrogen ions in solution based on reaction (4) (Higuchi et al.,

1953). This increase is most logically owing to the basic character of the amide linkage (-NH-CO-), resulting in the formation of a protonated intermediate due to Lewis acid base interaction (equation 4):



Thus, this acid-degraded positive complex of chloramphenicol and positive surface of fBC (zeta potential was positive) might repel each other and sorption of this degraded product was not favorable. At low pH, different chloramphenicol  $K_d$  values were obtained for biochar, fBC-1 and fBC-2, indicating that the degradation of chloramphenicol was not pronounced but comparable (Fig. 2). It can be concluded that sorption of chloramphenicol was mostly favoured by EDA interactions at low pH.

#### At pH 4.0 to 4.5

Chloramphenicol has three hydrogen bond donors and five hydrogen bond acceptor groups in its structure. Aqueous solution of chloramphenicol is neutral and hydrolysis does not occur rapidly at room temperature in the pH 2 to 7 range (Higuchi et al., 1953). We have carried out separate experiments for the dissociation of chloramphenicol at pH range from 1.5 to 10.0 and found that chloramphenicol concentration was almost same in all pH except only ~10% reduction at pH ~4.5. And this was might be due to the  $pK_a$  value of chloramphenicol. At pH 4.5, maximum  $K_d$  value is mostly due to electrostatic interactions. Proton exchange with water molecules is unfavorable (equation 5) by leaving the -OH group in solution, so the solution pH should increase (Ahmed et al., 2017b; Teixidó et al., 2011). However, in our experiments, the pH shifted towards the acidic region following adsorption. The proton transfer free energy was calculated using  $\Delta G_{H^+exch1}^0 = -RT \ln(K_{a1}/K_{aw})$  and found to be +45.5 kJ mol<sup>-1</sup>, where  $K_{aw}$  is the water dissociation constant for chloramphenicol. Furthermore, proton transfer is likely to be unfavorable by at least 15 kJ mol<sup>-1</sup> at 293 K and pH 5 (Teixidó et al., 2011; Pan et al., 2008). Thus, the decrease in equilibrium solution pH was due to release of proton from fBC-2 surface carboxylic groups ( $pK_a$  value ~4.0-5.0) as well as from chloramphenicol functional groups ( $pK_a$



value ~5.50) although deprotonation of water molecule release  $\text{OH}^-$  in the solution which might be neutralized by protons release from fBC-2 and chloramphenicol and the total interactions can be written as (Chloramphenicol  $\text{O}^- \cdots \cdots \text{H}^+ \cdots \cdots \text{OOC-fBC-2}$ ). Thus, overall the stabilization of the sorption complex can be obtained by releasing protons from surface functional groups and forming a strong CAHB. Hydrogen bonds among surface carboxylic groups, hydroxyl groups and quaternary nitrogen functional groups of fBC-2 and hydroxyl groups, nitro groups of chloramphenicol also play a major role in the maximum sorption at this pH (**case III, reaction 6**).



EAA interaction for  $\text{COOH}$  group may not occur within this pH range as  $\text{COOH}$  takes part in CAHB formation. Additionally, CAHB formation with the surface hydroxyl group of biochar was not possible due to higher  $pK_a$  value. It is noted that maximum sorption of any organic species is observed near a pH where  $pK_a$  lies within narrow limits. To test the  $\pi$ - $\pi$  EDA, EAA and EDD hypothesis, we also performed competitive effect on chloramphenicol sorption. The results are presented in Figs **6b** and **7**. It is noticeable that, fBC-2 surface functional groups such as  $\text{COOH}$  (due to matched  $pK_a$  value of surface  $\text{COOH}$  groups) and  $\text{C=O}$  can act as  $\pi$ -electron acceptor sites whereas arene unit can act as  $\pi$ -electron donor site (**Fig. 5**). Thus, in this case both interactions are preferable at this pH range if solutions are provided with both acceptor and donor competitors. Figure 6b clearly shows that PABA and phenanthrene strongly interacted with fBC-2 by suppressing chloramphenicol adsorption significantly. However, PABA was found to have comparative highly competitors than phenanthrene. This kind of interactions can be written simply as  $\pi$ - $\pi$  EDA interactions due to following reasons: PABA as acceptor and fBC-2 arene unit as donor; phenanthrene as donor and fBC-2 surface carboxylic groups and  $\text{C=O}$  groups as acceptor;  $\pi$ - $\pi$  EAA interactions due to PABA as acceptor and fBC-2 surface carboxylic groups and  $\text{C=O}$  as acceptor; and finally,  $\pi$ - $\pi$  EDD interactions due to

phenanthrene as donor and fBC-2 arene unit as donor. However, EDA interactions was the main reason with hydrogen bonds formations which can be confirmed from Fig. 7, which shows the strong adsorption of PABA and phenanthrene with fBC-2 due to EDA interactions that clearly support the previous explanations. Moreover, electrostatic attraction with opposite charged quadrupoles (fBC-2 as negative and  $\text{Ca}^{2+}$  as positive) were also observed as sorption of chloramphenicol reduce nearly ~18% in presence of  $0.005 \text{ M L}^{-1} \text{ CaCl}_2$  in the solution while presence of anion ( $\text{PO}_4^{3-}$ ) in solution did not bring any significance chloramphenicol sorption reduction.

Moreover, based on Raman spectra, it was found that the D to G band peak intensity ratio ( $I_D/I_G$ ) significantly decreased after sorption (Fig. 1b). This clearly indicated strong interaction among surface functional groups and chloramphenicol molecules. FTIR peak shifted to a point where C=O ( $\sim 1720 \text{ cm}^{-1}$ ) or  $-\text{COOH}$  functional groups ( $\sim 1028 \text{ cm}^{-1}$ ) as well as  $-\text{OH}$  groups ( $3400\text{-}3800 \text{ cm}^{-1}$ ) were located due to sorption of chloramphenicol onto functionalized biochar surfaces (Fig. 1a). Thus, maximum sorption of chloramphenicol in this pH range was due to the formation of CAHB and weak hydrogen bonds along with mainly EDA interactions in fBC.

#### ***At pH above 7.0***

At pH above 7.0,  $K_d$  values decreased when the pH of the solution was increased. However, the negatively charged biochar surface (zeta potential was highly negative) could still sorb chloramphenicol. This was mainly due to the formations of CAHB and weak hydrogen bonds among surface hydroxyl groups of biochar, aromatic nitro group and hydroxyl groups in chloramphenicol. The  $\text{p}K_a$  value of the surface hydroxyl group in carbon-based sorbents lay within 7-10. The only possible way was to form CAHB (Case IV, Fig. 5). EDA was not favorable at this pH since the hydroxyl group was deprotonated. In addition, EAA could be possible due to unchanged  $-\text{COOH}$  groups on the biochar surface (Case II, 1<sup>st</sup> part). To elucidate the EDA, EAA and EDD interaction mechanisms, competitors were introduced into solution at this pH range, and results (Figs 6c and 7) clearly showed that PABA and

phenanthrene had insignificant effect on the overall sorption of chloramphenicol. Hence, EDA, EAA and EDD interactions would have insignificant influence at this pH due to the fact that both surface hydroxyl groups of fBC-2 and phenanthrene acted as  $\pi$ -electron donor. Thus, their repulsive force was stronger than attractive forces. On the other hand, fBC-2 arene unit might function as  $\pi$ -electron donor site whereas chloramphenicol and PABA act as  $\pi$ -electron acceptor sites hence sorption of chloramphenicol remains stable (**Fig. 6c**). Interestingly, PABA sorption was significant in the absence of chloramphenicol. Hence, EDA might play a role in the overall sorption rather than EAA and EDD interactions. Moreover, the presence of anion ( $\text{PO}_4^{3-}$ ) in solution did not bring any significant increase in chloramphenicol sorption compared to without competitors. However, the presence of  $\text{Ca}^{2+}$  in solution caused a reduction in the sorption of chloramphenicol to some extent indicating the role of electrostatic attraction to oppositely charged ions (data not presented).

Based on the results of FTIR, chloramphenicol interacted with surface  $-\text{OH}$  which led to the increase of absorbance indicating the formations of hydrogen bonds. Moreover, the Raman spectra intensity band ratio ( $I_D/I_G$ ) also decreased suggesting that the  $-\text{OH}$  group played a major role in the sorption of chloramphenicol. As well, at high pH, chloramphenicol might also produce chloride ions in solution through hydrolysis (**equation 7**) (Higuchi et al., 1954).



Thus, chloramphenicol sorption at this pH range mainly occurred through hydrogen bond formation with little contribution from EDA interactions.

### 3.5. Application in different water at environmentally relevant concentrations

The fBC-2 was applied to remove chloramphenicol ( $3.10 \mu\text{M L}^{-1}$ ) from different water types. Pronounced differences in the removal efficiencies were observed for different water types in the sorption of chloramphenicol (**Fig. 8a**). However, synthetic wastewater had a highly negative influence on the overall removal of chloramphenicol by fBC-2 followed by lake and deionized

water. This might be due to the presence of different species (inorganic and organic) that were unfavorable for the comparative faster sorption of chloramphenicol from synthetic wastewater. For example, the presence of humic substances (discussed earlier) had negative influence on chloramphenicol sorption. Synthetic wastewater used in this study contained different organic materials (such as peptone, beef extract, humic acid, tannic acid, arabic acid, sodium lignin sulphonate, acacia gum powder) and inorganic ( $\text{KH}_2\text{PO}_4$  and  $\text{MgSO}_4 \cdot 3\text{H}_2\text{O}$ ) species. Thus, it was assumed that similar kinds of interactions with humic acid could happen in the case of synthetic wastewater. In addition to this, we have separately carried out chloramphenicol sorption experiments in the presence of sodium lignin sulphonate and acacia gum powder using the same synthetic wastewater composition and same conditions, and observed that the presence of these substances significantly hindered the sorption of chloramphenicol by ~50%. In comparison with deionized water, the removal of same amount of chloramphenicol from synthetic wastewater required a higher dosage of fBC-2 and also longer contact time (**Fig. 8a**). Control experiments in the absence fBC with different water matrices showed that there was no loss of chloramphenicol. On the other hand, fBC-2 needed less contact time and at a low dosage for the complete removal of chloramphenicol from lake water than synthetic wastewater. This indicated that lake water may contain fewer competitive ions or species than synthetic wastewater. In the case of deionized water, the removal of chloramphenicol was most effective which needed the least dosage of biochar. This is because deionized water does not contain any competitive species whether organic or inorganic. Hence the sorption of chloramphenicol was high and lower dosage of biochar was required. **The trend for removing environmentally relevant concentrations of chloramphenicol followed the order: deionized water > lake surface water > synthetic wastewater.** However, the removal of chloramphenicol from different water matrices can be improved by using higher concentration of biochar and by employing longer contact time (~48-60 h). Hence, fBC-2 can be successfully applied for the removal of environmentally relevant concentrations of chloramphenicol from water and wastewater.

### 3.6. Fingerprinting effect, regeneration and reusability of fBC-2

Chloramphenicol that was sorbed onto fBC-2 surface was desorbed using either methanol as solvent in order to regenerate fBC or, heated directly to regenerate fBC-2. The percentage of chloramphenicol desorption by methanol (two cycles on average) from fBC-2 was found to be ~91%, ~86% and ~89.2% for deionized water, synthetic wastewater and lake water, respectively (**Fig. A.1**). The results indicated that fBC-2 had specific sites or specific functional groups on its surface that interacted with chloramphenicol repeatedly, which clearly indicated some kind of “fingerprinting effect” (Westdijk et al., 2017). The successful cycles of application and desorption of chloramphenicol using fBC-2 showed almost the same results as those of virgin fBC-2.

This fingerprinting effect can be confirmed by the thermal regeneration studies of fBC-2. For this reason, fBC-2 was thermally regenerated and tested under the same conditions as freshly prepared fBC-2. Regeneration ability was repeated for six cycles and it emerged that fBC-2 can maintain excellent reusability with undiminished removal efficiencies (almost 100% under same contact time and same dosages) up to the 6<sup>th</sup> cycle of application (**Fig. 8b**). It is evident that due to thermal regeneration, chloramphenicol antibiotic was sorbed onto specific sites or with specific functional groups (-OH, -COOH or -C=O groups confirmed by Raman spectra) of fBC-2. This can be explained by two facts. Firstly, chloramphenicol molecules that were sorbed onto the fBC-2 surface or functional groups had to emerge during thermal treatment and leave the functional groups or surface intact as they were before. Therefore, further application of regenerated fBC-2 for chloramphenicol sorption was accelerated. Secondly, thermal regeneration of fBC-2 at 300 °C might have created some new binding sites which may have accelerated the sorption process. However, this kind of outcome might not be significant since the functionalization of biochar was carried out at 600 °C and an increase in surface porosity theoretically may not be feasible below that temperature. Furthermore, no

significant change in biochar weight was noticed after regeneration. So, it can be suggested that chloramphenicol sorption on fBC-2 was highly site specific producing a **fingerprinting** effect, which was favorable for chloramphenicol removal and subsequent regeneration for repeatable applications.

From the findings it can be stated that fBC-2 can be successfully regenerated and reused for complete sorption of chloramphenicol. This type of functionalization of different carbonaceous materials is very efficient for the removal of organic contaminants from water and wastewater. Previous study also confirmed the efficient removal of three sulfonamide antibiotics in single and competitive modes (Ahmed et al., 2017b) using fBC. In addition, fBC-2 or the functionalization of other carbonaceous materials utilizing the same method can generate more cost effective sorbents for the removal of different types of emerging organic contaminants.

#### 4. Conclusions

The sorptive removal of chloramphenicol by fBC was very effective in different water types. The removal of chloramphenicol was pH dependent and maximum sorption occurred in the pH 4.0-4.5 range. The removal of chloramphenicol was described better by the Langmuir isotherm model than the Freundlich isotherm model. Sorption of chloramphenicol onto fBC-2 was significantly influenced by humic acid, salt concentration and different water properties. The removal of chloramphenicol was higher in deionized water followed by lake water and synthetic wastewater.  $K_d$  was decreased by ~70% when humic acid concentration was increased from 0.5 to 40 mg L<sup>-1</sup>. The presence of low concentration of salts and soil resulted in increasing  $K_d$  values while high concentration of salts and soil led to decreasing  $K_d$  values. The sorption of chloramphenicol onto fBC involved mainly **EDA interactions at pH < 2.0**; formation of CAHB and hydrogen bonds in addition to EDA in the pH 4.0-4.5; and CAHB and EDA interactions at pH > 7.0. fBC-2 can be regenerated with excellent reusability up to many cycles for the efficient

removal of chloramphenicol due to creating the fingerprint effect onto specific sites of fBC-2. Finally, fBC-2 or functionalization of other carbonaceous materials with the same method can potentially generate better sorbents for the removal of similar organic contaminants in a sustainable manner.

## Acknowledgements

We thank UTS for a PhD scholarship, and New Forest Asset Management Pty Ltd, Portland, Victoria, Australia for donating *Eucalyptus Globulus* wood sample.

## References

- Ahmed M. B., Zhou J. L., Ngo H. H., Guo W., 2015. Adsorptive removal of antibiotics from water and wastewater: Progress and challenges. *Sci. Total Environ.* 53, 112-126.
- Ahmed M. B., Zhou J. L., Ngo H. H., Guo W., 2016a. Insight into biochar properties and its cost analysis. *Biomass Bioenerg.* 84, 76-86.
- Ahmed M. B., Zhou J. L., Ngo H. H., Guo W., Chen M., 2016b. Progress in the preparation and application of modified biochar for improved contaminant removal from water and wastewater. *Bioresour. Technol.* 214, 836-851.
- Ahmed M. B., Zhou J. L., Ngo H. H., Guo W., Thomaidis N.S., Xu J., 2017a. Progress in the biological and chemical treatment technologies for emerging contaminant removal from wastewater: a critical review. *J. Hazard. Mater.* 323, 274-298.
- Ahmed M. B., Zhou J. L., Ngo H. H., Guo W., Johir M. A. H., Sornalingam K., 2017b. Single and competitive sorption properties and mechanism of functionalized biochar for removing sulfonamide antibiotics from water. *Chem. Eng. J.* 311, 348-358.
- Ahmed M. B., Zhou J. L., Ngo H. H., Guo W., Johir M. A., Sornalingam K., Belhaj D., Kallel M. 2017c. Nano-Fe<sup>0</sup> immobilized onto functionalized biochar gaining excellent stability

589 during sorption and reduction of chloramphenicol via transforming to reusable magnetic  
 590 composite. Chem. Eng. J. 322, 571-581.

591 Boxall A.B., Kolpin D.W., Halling-Sørensen B., Tolls J., 2003. Peer reviewed: are veterinary  
 592 medicines causing environmental risks? Environ. Sci. Technol. 37, 286A-294A.

593 Chen C.Q., Zheng L., Zhou J.L., Zhao, H., 2017. Persistence and risk of antibiotic residues and  
 594 antibiotic resistance genes in major mariculture sites in Southeast China. Sci. Total  
 595 Environ. 580, 1175-1184.

596 Chen J., Zhang D., Zhang H., Ghosh S., Pan B., 2016. Fast and slow adsorption of  
 597 carbamazepine on biochar as affected by carbon structure and mineral composition. Sci.  
 598 Total Environ. 579, 598-605.

599 Chen K., Zhou J.L., 2014. Occurrence and behavior of antibiotics in water and sediments from  
 600 the Huangpu River, Shanghai, China. Chemosphere 95, 604-612.

601 Cornelissen G., and Gustafsson Ö., 2005. Importance of unburned coal carbon, black carbon,  
 602 and amorphous organic carbon to phenanthrene sorption in sediments. Environ. Sci.  
 603 Technol. 39, 764-769.

604 Dai J., He J., Xie A., Gao L., Pan J., Chen X., Zhou Z., Wei X., Yan Y., 2016. Novel pitaya-  
 605 inspired well-defined core-shell nanospheres with ultrathin surface imprinted nanofilm  
 606 from magnetic mesoporous nanosilica for highly efficient chloramphenicol removal. Chem.  
 607 Eng. J. 284, 812-822.

608 Dai Z., Zhang X., Tang C., Muhammad N., Wu J., Brookes P.C., Xu J., 2017. Potential role of  
 609 biochars in decreasing soil acidification - a critical review. Sci. Total Environ. 581-582,  
 610 601-611.

611 Das O., Sarmah A.K. 2015. The love-hate relationship of pyrolysis biochar and water: a  
 612 perspective. Sci. Total Environ. 512, 682-685.



613 Fan Y., Wang B., Yuan S., Wu X., Chen J., Wang L., 2010. Adsorptive removal of  
614 chloramphenicol from wastewater by NaOH modified bamboo charcoal. *Bioresour.*  
615 *Technol.* 101(19), 7661-7664.

616 Higuchi T., Bias C. D., 1953. The kinetics of degradation of chloramphenicol in solution: I. a  
617 study of the rate of formation of chloride ion in aqueous media, *J. Am. Pharm. Assoc.* 42,  
618 707-714.

619 Higuchi T., Marcus A. D., 1954. The kinetics of degradation of chloramphenicol in solution:  
620 III. The nature, specific hydrogen ion catalysis, and temperature dependencies of the  
621 degradative reactions, *J. Am. Pharm. Assoc.* 43, 530-535.

622 Ji L., Chen W., Duan L., Zhu D., 2009a. Mechanisms for strong adsorption of tetracycline to  
623 carbon nanotubes: a comparative study using activated carbon and graphite as adsorbents.  
624 *Environ. Sci. Technol.* 43, 2322-2327.

625 Ji L., Chen W., Zheng S., Xu Z., Zhu D., 2009b. Adsorption of sulfonamide antibiotics to  
626 multiwalled carbon nanotubes. *Langmuir* 25, 11608-11613.

627 Ji L., Wan Y., Zheng S., Zhu D., 2011. Adsorption of tetracycline and sulfamethoxazole on  
628 crop residue-derived ashes: implication for the relative importance of black carbon to soil  
629 sorption. *Environ. Sci. Technol.* 45, 5580-5586.

630 Keiluweit M., Kleber M., 2009. Molecular-level interactions in soils and sediments: The role  
631 of aromatic  $\pi$ -systems. *Environ. Sci. Technol.* 43, 3421-3429.

632 Lattao C., Cao X., Mao J., Schmidt-Rohr K. Pignatello J. J., 2014. Influence of molecular  
633 structure and adsorbent properties on sorption of organic compounds to a temperature series  
634 of wood chars. *Environ. Sci. Technol.* 48, 4790-4798.

635 Lehmann J., and Joseph S. (Eds.), 2015. Biochar for environmental management: science,  
636 technology and implementation. Routledge.

637 Liao P., Zhan Z., Dai J., Wu X., Zhang W., Wang K., Yuan S., 2013. Adsorption of tetracycline  
638 and chloramphenicol in aqueous solutions by bamboo charcoal: A batch and fixed-bed  
639 column study. *Chem. Eng. J.* 228, 496-505.

640 Lofrano G., Libralato G., Adinolfi R., Siciliano A., Iannece P., Guida M., Giugni M., Ghirardini  
641 A.V., Carotenuto M., 2016. Photocatalytic degradation of the antibiotic chloramphenicol  
642 and effluent toxicity effects. *Ecotox. Environ. Safe.* 123, 65-71.

643 Ma X., Agarwal S., 2016. Adsorption of emerging ionizable contaminants on carbon nanotubes:  
644 advancements and challenges. *Molecules* 21, (5), 628.

645 Mandal A., Singh N., Purakayastha, T.J., 2017. Characterization of pesticide sorption behaviour  
646 of slow pyrolysis biochars as low cost adsorbent for atrazine and imidacloprid removal. *Sci.*  
647 *Total Environ.* 577, 376-385.

648 Maskaoui K., Zhou J.L., 2010. Colloids as a sink for certain pharmaceuticals in the aquatic  
649 environment. *Environ. Sci. Pollut. Res.* 17, 898-907.

650 Mi L., Licina G. A., Jiang S., 2014. Nonantibiotic-based pseudomonas aeruginosa biofilm  
651 inhibition with osmoprotectant analogues. *ACS Sustain. Chem. Eng.* 2(10), 2448-2453.

652 Nie M., Yan C., Li M., Wang X., Bi W., Dong W., 2015. Degradation of chloramphenicol by  
653 persulfate activated by  $\text{Fe}^{2+}$  and zerovalent iron. *Chem. Eng. J.* 279, 507-515.

654 Pan B., Xing B., 2008. Adsorption mechanisms of organic chemicals on carbon nanotubes.  
655 *Environ. Sci. Technol.* 42, 9005-9013.

656 Park S., Lee K. S., Bozoklu G., Cai W., Nguyen S. T., Ruoff R. S., 2008. Graphene oxide  
657 papers modified by divalent ions—enhancing mechanical properties via chemical cross-  
658 linking. *ACS nano*, 2(3), 572-578.

659 Peng B., Chen L., Que C., Yang K., Deng F., Deng X., Shi G., Xu G., Wu M., 2016. Adsorption  
660 of antibiotics on graphene and biochar in aqueous solutions induced by  $\pi$ - $\pi$  interactions,  
661 *Sci. Rep.* 6, 31920.

662 Pignatello J. J., Kwon S. Lu Y., 2006. Effect of natural organic substances on the surface and  
 663 adsorptive properties of environmental black carbon (char): attenuation of surface activity  
 664 by humic and fulvic acids. *Environ. Sci. Technol.* 40, 7757-7763  
 665 Qin L., Zhou Z., Dai J., Ma P., Zhao H., He J., Xie A., Li C., Yan Y., 2016. Novel N-doped  
 666 hierarchically porous carbons derived from sustainable shrimp shell for high-performance  
 667 removal of sulfamethazine and chloramphenicol. *J. Taiwan Inst. Chem. Eng.* 62, 228-238.  
 668 Sander, M., Pignatello, J. J., 2005. Characterization of charcoal adsorption sites for aromatic  
 669 compounds: Insights drawn from single-solute and bi-solute competitive experiments.  
 670 *Environ. Sci. Technol.* 39, 1606-1615.  
 671 Sorrenti G., Masiello C. A., Dugan B., Toselli M., 2016. Biochar physico-chemical properties  
 672 as affected by environmental exposure. *Sci. Total Environ.* 563, 237-246.  
 673 Suliman W., Harsh J. B., Abu-Lail N. I., Fortuna A. M., Dallmeyer I., Garcia-Pérez M. 2017.  
 674 The role of biochar porosity and surface functionality in augmenting hydrologic properties  
 675 of a sandy soil. *Sci. Total Environ.* 574, 139-147.  
 676 Taheran M., Naghdi M., Brar S.K., Knystautas E.J., Verma M., Ramirez A.A., Valero J.R.,  
 677 2016. Adsorption study of environmentally relevant concentrations of chlortetracycline on  
 678 pinewood biochar. *Sci. Total Environ.* 571, 772-777.  
 679 Teixidó M., Pignatello J.J., Beltrán J. L., Granados M., Peccia J., 2011. Speciation of the  
 680 ionizable antibiotic sulfamethazine on black carbon (biochar). *Environ. Sci. Technol.*  
 681 45(23), 10020-10027.  
 682 Westdijk J., Metz B., Spruit N., Tilstra W., van der Gun J., Hendriksen C., Kersten G., 2017.  
 683 Antigenic fingerprinting of diphtheria toxoid adsorbed to aluminium phosphate.  
 684 *Biologicals*, 47, 69-75.  
 685 Wu D., Chen Y., Zhang Z., Feng Y., Liu Y., Fan J., Zhang Y., 2016. Enhanced oxidation of  
 686 chloramphenicol by GLDA-driven pyrite induced heterogeneous Fenton-like reactions at  
 687 alkaline condition. *Chem. Eng. J.* 294, 49-57.

688 Xia S., Gu Z., Zhang Z., Zhang J., Hermanowicz S.W., 2016. Removal of chloramphenicol  
689 from aqueous solution by nanoscale zero-valent iron particles. *Chem. Eng. J.* 257, 98-104.

690 Zhang M., Shu L., Guo X., Shen X., Zhang H., Shen G., Wang X., 2015. Impact of humic acid  
691 coating on sorption of naphthalene by biochars. *Carbon* 94, 946-954.

692 Zhao H., Zhang J., Zhou J.L., 2015. Tidal impact on the dynamic behavior of dissolved  
693 pharmaceuticals in the Yangtze Estuary, China. *Sci. Total Environ.* 536, 946-954.

694 Zhou F., Wang H., Fang S., Zhang W., Qiu R., 2015. Pb(II), Cr(VI) and atrazine sorption  
695 behavior on sludge-derived biochar: role of humic acids. *Environ. Sci. Pollut. Res.* 22,  
696 16031-16039.

697 Zhu D., Hyun S., Pignatello J.J., Lee L.S., 2004. Evidence for  $\pi$ - $\pi$  electron donor-acceptor  
698 interactions between  $\pi$ -donor aromatic compounds and  $\pi$ -acceptor sites in soil organic  
699 matter through pH effects on sorption. *Environ. Sci. Technol.* 38(16), 4361-4368.

700 Zhu D., Kwon S. Pignatello, J.J., 2005 Adsorption of single-ring organic compounds to wood  
701 charcoals prepared under different thermochemical conditions. *Environ. Sci. Technol.* 39,  
702 3990-3998.

703 Zhu D., Pignatello J.J., 2005. Characterization of aromatic compound sorptive interactions with  
704 black carbon (charcoal) assisted by graphite as a model. *Environ. Sci. Technol.* 39, 2033-  
705 2041.

706 Zhu Z., Xie J., Zhang M., Zhou Q., Liu F., 2016. Insight into the adsorption of PPCPs by porous  
707 adsorbents: effect of the properties of adsorbents and adsorbates. *Environ. Pollut.* 214, 524-  
708 531.